Green and Red Fluorescent Proteins: Photo- and Thermally Induced Dynamics Probed by Site-Selective Spectroscopy and Hole Burning

S. Bonsma,[a] R. Purchase,[a] S. Jezowski,[a] J. Gallus,[a] F. Könz,[a] and S. Völker*[a, b]

The cloning and expression of autofluorescent proteins in living matter, combined with modern imaging techniques, have thoroughly changed the world of bioscience. In particular, such proteins are widely used as genetically encoded labels to track the movement of proteins as reporters of cellular signals and to study protein–protein interactions by fluorescence resonance energy transfer (FRET). Their optical properties, however, are complex and it is important to understand these for the correct interpretation of imaging data and for the design of new fluorescent mutants. In this Minireview we start with a short survey of the field and then focus on the photo- and thermally induced dynamics of green and red fluorescent proteins. In particular, we show how fluorescence line narrowing and high-resolution spectral hole burning at low temperatures can be used to unravel the photophysics and photochemistry and shed light on the intricate electronic structure of these proteins.

1. Introduction

In the past decade green fluorescent proteins (GFPs) have become indispensable in molecular and cell biology as noninvasive luminescent labels for monitoring gene expression, protein localization and protein interactions by fluorescence microscopy.[1–8] Although native GFP from the jellyfish *Aequorea victoria* had been investigated for 30 years,[1] the breakthrough came in 1992 when it was cloned[9] and it was subsequently discovered that the visible fluorescence is genetically encodable.[10a] Because no external cofactors or substrates other than molecular oxygen are required for the formation of the fluorescent chromophore,[1] the c-DNA encoding GFP can be fused to the DNA of virtually any protein of interest and, once expressed, it folds independently of the protein to which it is fused, becoming a strong *in vivo* fluorescent label.[10a,b] The chromophore of GFP responsible for its strong green fluorescence is formed autocatalytically from three amino acid residues of the protein backbone.[11–13]

The engineering of GFP mutants of different colors (from blue to yellow), having more brightness, improved folding and photostability,[1,7,12–16] and the recent development of pH-sensitive variants of GFP[17a,b] and photoactivatable or "kindling" GFPs,[8,18–20] in combination with advanced fluorescence imaging techniques,[5,8] have stimulated the use of GFPs for studying the simultaneous localization and dynamics of two and more fusion proteins,[21] even at the level of single cells.[20,22] Also tumor cells expressing GFP *in vivo* are now successfully being transplanted into animals and their growth and metastasis visualized by whole-body imaging in major organs.[23]

A further breakthrough has been the cloning of a red fluorescent protein (DsRed) from the non-bioluminescent sea coral *Discosoma sp* and of the mutants of DsRed.[24,25] These red fluorescent proteins (RFPs) have attracted renewed interest, not only because of their dramatic red-shifted emission, but also as potential fusion partners of GFP mutants for creating donor–acceptor pairs to follow protein–protein interactions by fluorescence resonance energy transfer (FRET).[7,21,26] One of the advantages of DsRed is that its strong, orange-red emission does not overlap with the green autofluorescence of cells when used inside living organisms. DsRed, however, has two major drawbacks: a strong tendency to form oligomers and a slow maturation.[27] These problems have recently been overcome by creating faster maturing mutants[28] and a monomer of DsRed.[7,29]

The structures of wt-GFP[30] and several of its mutants (GFPs),[15,31] as well as those of DsRed[32] and some of its mutants (RFPs),[33] have been resolved by X-ray crystallography. GFPs and RFPs are small, 25–30 kDa single-chain proteins with 220–240 amino acid residues, forming an 11-stranded β-barrel (with dimensions of about 3 nm × 4 nm). Inside the barrel, an α-helix contains the sequence of three residues from which the chromophore (a *p*-hydroxy-benzylidene-imidazolinone) is derived. The chromophore, a fluorescent π–π^* electron system, is protected from the bulk solvent and rigidly held within the barrel. On going from GFP to RFP, the π–π^* system is more extended and a large red-shift of the spectrum results. The emission of autofluorescent proteins covers a range from $\approx$440 to 649 nm.[1,7,25,34]

[a] *S. Bonsma, Dr. R. Purchase, S. Jezowski, Dr. J. Gallus,[+] Dr. F. Könz,[++] Prof. Dr. S. Völker*
Huygens and Gorlaeus Laboratories, Leiden University
P.O. Box 9504, 2300 RA Leiden (The Netherlands)
Fax: (+31) 71-527-5819
E-mail: silvia@molphys.leidenuniv.nl

[b] *Prof. Dr. S. Völker*
Department of Biophysics, Vrije Universiteit, De Boelelaan 1081, 1081 HV Amsterdam (The Netherlands)

[+] *Current address:*
MEOS AG, Hartheimer Str.15, 79427 Eschbach (Germany)

[++] *Current address: Technical High School Stord/Haugesund*
P.O. Box 5000, 5409, Stord (Norway)

  DOI: 10.1002/cphc.200500005

Despite the known structure and the understanding of the basic processes underlying the fluorescence of GFPs and RFPs, there are still many unanswered questions regarding their photophysics and photochemistry, both from a theoretical and an experimental point of view.[35,36] One of these puzzles, for example, is to figure out how to obtain real "one-color" GFPs, that is, with only one photostable conformation. So far, GFPs have proven to exist in various photo-interconvertible forms.[37,38] Related to this puzzle is that of the relative energies of these forms and the barrier heights between them, problems that have hardly been discussed in the literature[3] and will be treated here.

The relation between the structure and the optical properties of the GFP chromophore, either in the protein or in solution, has been considered by a number of groups. For example, quantum mechanical modelling of the GFP chromophore and its near environment and ab initio relaxation-path calculations have been reported with the aim of determining the mechanisms underlying the fluorescence.[35,36,39] Also a broad set of spectroscopic techniques has been applied. Many papers deal with ultrafast (femto- to picosecond) absorption and fluorescence spectroscopy on GFPs[17a,40] or on the isolated chromophore in solution.[41] It is remarkable that at ambient temperature both the chromophore in solution and denatured GFPs show almost no fluorescence, whereas renaturated GFPs and the model chromophore frozen to 77 K are highly fluorescent.[40c,41a,41d,42] A *cis–trans* isomerization has been proposed as a possible mechanism for the radiationless relaxation of the chromophore in solution.[6,36,39a,40c,41a,41d,42a] A number of papers dealing with the photophysics of protonated and deprotonated model chromophores of GFP in the gas phase have also been reported;[43] only a few applications of NMR spectroscopy related to conformational changes in a GFP mutant have appeared so far.[44] Specific interactions between the protein and the chromophore in the ground state, for example, the decarboxylation of Glu 222 on strong UV irradiation of wt-GFP, have been studied by Fourier-transform infrared (FTIR)[45a] and optical spectroscopy combined with crystallography.[45b] Vibrational properties of the ground states of GFPs and model chromophores in their neutral and anionic forms have further been unravelled by Raman spectroscopy,[46] and complemented by ab initio calculations on the isolated chromophore.[47]

GFPs exhibit a complex photophysical behavior, not only in the ensemble but also at the single-molecule (SM) level.[48] A few reviews on SM optical spectroscopy and microscopy of autofluorescent proteins have appeared in the literature;[49] the reader is referred to them for further details. Applications of SM to live-cell imaging microscopy, in particular a discussion on photophysical parameters for a selection of autofluorescent proteins and the imaging of single Ca^{2+} channels in live cells, can be found in refs. [50a,b]. Another technique related to SM that provides useful dynamical information on conformational changes in small ensembles of molecules in solution in the micro-to-millisecond time span is fluorescence correlation spectroscopy (FCS).[51]

In this Minireview we focus on the photophysics of green and red fluorescent proteins[37,38,52,53] studied by site-selective, high-resolution optical spectroscopy and hole burning.[54] After introducing the methods in Section 2, we demonstrate what can be learnt with these techniques using a few examples. The first example is wild-type (wt) GFP. In Sections 3.1 and 3.2 we explain how its hidden intermediate I form was identified by hole burning at very low temperature[37] and by site-selective excitation and emission spectroscopy at ambient temperatures. We further show how the 0–0 transitions of three forms of wt-GFP have been determined and the pathways of photo-interconversion unravelled, leading to an energy-level diagram.[37] By studying three mutants of GFP, it was subsequently discovered in our laboratory[38] that the behavior of wt-GFP is more general: in contrast to what had previously been believed, these mutants are not photostable "one-colour" systems, but display reversible photoconversions between at least three conformations.[38]

In Section 4, we present the photo- and thermally induced dynamics of the red fluorescent protein DsRed. We discovered that a number of conformations absorbing and emitting at different colors can be photoinduced at low temperatures and we identified their 0–0 transitions.[52] From the evolution of the emission spectra with burning time, we further proved that energy transfer takes place between these forms[52] (Section 4.1). In addition, we determined the ground-state energy differences and energy-barrier heights between the various conformations from temperature-dependent excitation and fluorescence spectroscopy[52] (Section 4.2). Finally, intrigued by the fact that the chromophores of GFPs and RFPs are intrinsically built into the protein chain, we studied the optical dephasing of DsRed by megahertz-resolution hole burning and determined the homogeneous linewidth—to our knowledge, the first result of this kind reported for any GFP[53] (Section 4.3). We further present the spectral distribution of "trap" molecules, that is, those molecules that cannot undergo energy transfer, and discuss the implications of the ensuing electron–phonon coupling strength in relation to the structure of autofluorescent proteins.

2. Site-Selective Spectroscopy and Hole Burning: Principles and Applications

The results to be presented in Sections 3 and 4 have been obtained by site-selective spectroscopy—also called fluorescence line narrowing (FLN)—and hole burning (HB).[54] FLN and HB at low temperature yield an increase of spectral resolution of a factor of 10^3–10^5 compared to conventional optical spectroscopy at room temperature. The reason is that thermal broadening is suppressed and narrow-band lasers are used together with high-resolution monochromators. Two types of information can be retrieved from such experiments that otherwise remain hidden in the spectra. First, one obtains a "fingerprint" of the species (conformers) involved. These fingerprints are provided by the origins (0–0 transitions) identified in the spectra and by the vibronic structure. In this manner, energy-level schemes and pathways of photoconversion can be constructed from the low-temperature experiments, which provide essential constraints when interpreting room-temperature results.

Second, from the homogeneous linewidth Γ_{hom} one can extract quantitative information on dynamical processes such as decay times and interactions between chromophores or a chromophore and its environment.[54]

In site-selection (or FLN) spectroscopy ,[54] a sub-ensemble of molecules within the inhomogeneously broadened absorption band is selectively excited with a narrow-band laser and detected with a high-resolution monochromator and/or Fabry-Pérot etalon. The principle of the method is explained in Figure 1 a. In emission spectroscopy (left), the vibrational levels ν_{0i} of the ground state are obtained, whereas excitation spectroscopy (right) yields those of the excited state ν_{1i}. FLN also enables the identification of the onset of "downhill" energy transfer within the absorption spectrum[53,54c–56] (see Section 4.3).

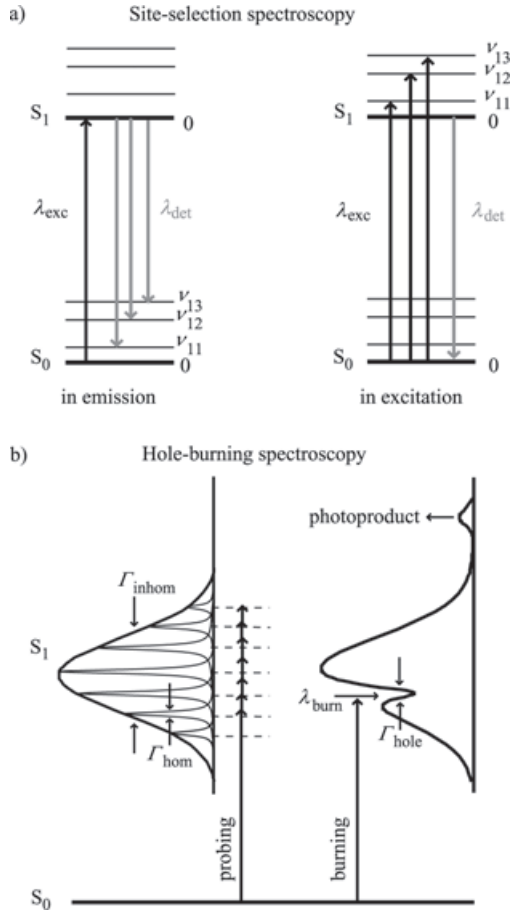

Figure 1. *a) Energy-level schemes representing the principle of site selection (also called fluorescence line narrowing) spectroscopy in emission (left) and excitation (right). In emission, the laser wavelength λ_{exc} (black arrow) is fixed at the 0–0 transition (where no phonon sidebands are excited) and the detection wavelength λ_{det} is scanned with a high-resolution monochromator over the vibrational levels of the ground state (grey arrows). In excitation, the detection wavelength λ_{det} is fixed at the 0–0 transition (grey arrow) and the laser wavelenght λ_{exc} is scanned over the vibrational levels of the first electronically excited state (black arrows). Information is obtained on vibrational frequencies ν_{0n} of the ground state (left) and of the excited state ν_{1n} (right).[54] b) Schematic representation of the hole-burning process. Left: Diagram of an inhomogeneously broadened absorption band of width Γ_{inhom}. The homogeneous bands of width Γ_{hom} of the individual electronic transitions are hidden under the broad inhomogeneous absorption band. Right: Spectral hole burnt with a narrow-band laser at wavelength λ_{burn}. The molecules resonant with the laser wavelength undergo a photoreaction creating a "hole" in the absorption band. This hole is subsequently probed by scanning the laser over the wavelength range of interest. The photoproduct absorbs at a different wavelength, usually outside the inhomogeneous band.[54]*

Spectral hole burning (HB) is a powerful tool for spectroscopy in the megahertz regime. Because it yields the homogeneous linewidth Γ_{hom}, information can be obtained on the rates of population relaxation processes such as decay and energy transfer (so-called T_1 processes) and of optical dephasing and spectral diffusion (so-called T_2 processes)[53,54] (Section 4.3). As we shall see below HB also permits the accurate identification of 0–0 transitions in inhomogeneously broadened spectra.

The procedure for "burning" spectral holes is described in the caption of Figure 1 b. The width of the hole, under the condition that the laser bandwidth is much smaller than Γ_{hom}, is proportional to the homogeneous linewidth Γ_{hom}[53,54] (Section 4.3). The mechanisms causing HB can be divided into two general categories: persistent HB and transient HB (THB). Within the first category, one can distinguish again between photochemical HB (PHB) and non-photochemical HB (NPHB). The time scales involved in PHB and NPHB are usually seconds to minutes, whereas in THB they are often micro- or milliseconds. It is important to realize that the hole widths determining the value of Γ_{hom} dependent only on the T_1- and T_2-type dynamic processes of interest, but are independent of the HB mechanism.[54] HB has also proven useful for getting the vibrational frequencies of the excited state. In this case, a hole is burnt in the zero-phonon line region and many satellite holes will appear in the excitation spectrum at positions given by the vibrational frequencies of the excited state.[54]

In green and red fluorescent proteins, persistent holes arise from photoinduced conformational changes involving neutral (protonated) and anionic (deprotonated) forms of the chromophore.[37,38,52,53] In some cases, the photoproducts absorb far away from the original molecule (thousands of cm^{-1}) and in others they have their absorption bands much nearer (a few hundred cm^{-1}; Sections 3.1 and 4.1). Also electron–phonon coupling strengths can be obtained by HB[37,53,56] (Section 4.3).

3. Green Fluorescent Proteins (GFPs)

The green fluorescent protein (wt-GFP) of the jellyfish *Aequorea victoria* consists of 238 amino acids[1–9] in a single chain folded into a so-called "β-barrel"[14b,30,31] (Figure 2 a, left). Inside the β-barrel and buried in its center sits the fluorescent chromophore (Figure 2 a, right). It forms part of the protein chain and originates from an autocatalytic cyclization and subsequent oxidation of three amino acids residues of the protein: serine (Ser)-65, tyrosine (Tyr)-66 and glycine (Gly)-67.[1,12,13,42a] The chromophore consists of a phenolic and an imidazolidinone ring rigidly held within the β-barrel, forming a fluorescent π–π* electron system[1–6] protected from the bulk solvent. The surrounding cavity has a number of charged residues in the vicinity of the chromophore and four water molecules that are important in establishing a hydrogen-bonding network around it. This network is critical in determining the spectroscopic and photochemical properties of GFP.[3,35,36]

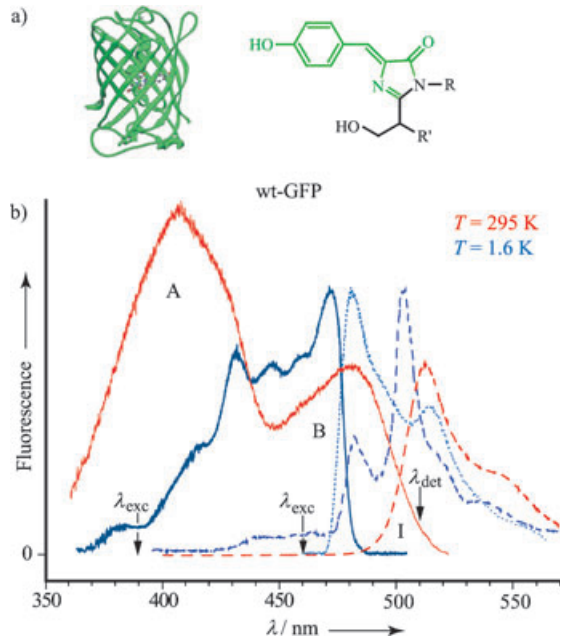

Figure 2. *wt-GFP. a) The "β-barrel" crystal structure (left) and the chromophore (right). b) Excitation spectra (solid lines) and emission spectra (dashed and dotted lines) at 295 K (red curves) and 1.6 K (blue curves). The excitation spectra were detected at 510 nm. The emission spectra were selectively excited in the A form (dashed lines) at 390 nm and the B form (dotted line) at 460 nm. The emission maxima at ≈480 nm (1.6 K, blue dashed and dotted lines) belong to the B form, while the maxima at 501 nm (1.6 K, blue dashed lines) and 508 nm (295 K, red dashed line) correspond to emission from the I form. The absolute intensities of the various spectra are not drawn to a common scale.*

The room-temperature excitation (or absorption) spectrum of wt-GFP is characterized by two maxima (Figure 2b, red, solid line) which have been attributed to different protonation states of the chromophore: the band at ≈398 nm to a neutral (protonated) A form and the band at ≈478 nm to an anionic (deprotonated) B form.[31b,40a,40b,57] On excitation at ≈400 nm, the emission spectrum of wt-GFP at 295 K shows a strong, green fluorescence at ≈508 nm (Figure 2b, red dashed line).[13,15,57] From picosecond time-resolved spectroscopy studies at room temperature and 77 K[40a,b] it was concluded in 1996 that on excitation of A to A*, a proton transfer occurs to an excited intermediate state I*. It was further proposed in refs. [40a,b] that the majority of the molecules excited to I* decay by emitting the strong, green fluorescence at ≈508 nm, while a minor fraction photoconverts to B. In this model, I* and I were assumed to be unrelaxed forms of B* and B. However, whether an I form in its ground state existed remained unclear at the time.[31b,c,40a,40b] We shall consider evidence for the existence of a distinct I form, not only at low temperature but also at room temperature.

3.1. wt-GFP: Identification of the I Form at Liquid-Helium Temperature

The I form in the ground state of wt-GFP was identified in 1999 in our laboratory by means of high-resolution, site-selective spectroscopy and hole burning.[37] Here we shortly discuss the results and first consider Figure 2b. Upon cooling from 295 K to 1.6 K, the excitation and emission spectra of wt-GFP become narrower and more structured (red versus blue curves); moreover the ratio of the intensities of the A and B forms inverts. Under the assumption that the quantum yield of fluorescence (Φ_{fl}) remains constant, or that the decrease of Φ_{fl} with increasing temperature is the same for both forms, the inversion is an indication for thermodynamic equilibrium with B having a slightly lower ground-state energy than A. Particularly relevant is that the broad wing on the red side of the spectrum at 295 K (red trace) disappears at 1.6 K (blue trace). We attributed this red wing to the I form and postulated that this form should be present at room temperature but absent at 1.6 K, and thus the ground-state energy of I has to be somewhat higher than that of A and B.[37] We have corroborated that the I form is indeed thermally populated at 295 K (see Section 3.2 and Figure 4). When comparing the excitation and emission spectra at 295 K (red curves) and 1.6 K (blue curves), we notice that the spectra intersect at ≈500 nm at 295 K, and at ≈477 nm at 1.6 K. If only A and B were present in the ground state at room temperature, one would not expect such an appreciable shift as a function of temperature. The emission spectrum at 295 K (red dashed line) supports the suggestion[40a,b] that on excitation into the A form at ≈400 nm, the excited state A* rapidly photoconverts into I*, which then emits at ≈508 nm.

At 1.6 K, the bands originating from B and B* (solid and dotted blue curves in Figure 2b) are rather mirror symmetric about their 0–0 transition (at 477 nm), having a small Stokes shift $\Delta = 220 \pm 10\ cm^{-1}$. Remarkable is the strong variation in the shape of the emission spectra with excitation wavelength (λ_{exc}). For $\lambda_{exc} \leq 434$ nm (the 0–0 transition of A, see Figure 3b and discussion below), both the A and B forms are excited (blue dashed curve in Figure 2b; the weak emission in the 440–460 nm region results from transitions from A* to vibrational levels of A). Under these excitation conditions, the excited-state proton transfer process A*→I* occurs and the emission spectrum exhibits strong fluorescence from I* and weaker from B* (dashed curve in Figure 2). The emission from I* at 1.6 K is blue-shifted with respect to that at ambient temperature by ≈7 nm (compare blue and red dashed curves in Figure 2b). The emission peak at 482 nm belonging to B* is also observed for $\lambda_{exc} > 434$ nm, where only the B form is excited and emits (dotted blue curve in Figure 2b and energy-level scheme in Figure 3b). By recording high-resolution spectra at 1.6 K systematically as a function of λ_{exc} and λ_{det}, we have identified vibrational frequencies between ≈200 and ≈1700 cm^{-1} in the ground and excited states of the three forms of wt-GFP.[37] The values reported in ref. [37] for the ground states are consistent with the more accurate determination by Raman spectroscopy in the region of ≈1000–1700 cm^{-1}[46a,b] and 400–1000 cm^{-1}.[46e] In the Raman experiments, the I form was not considered.

Using hole burning as a diagnostic tool, we discovered that the various forms of wt-GFP can be photo-interconverted.[37] This is illustrated at the left of Figure 3a, which shows excita-

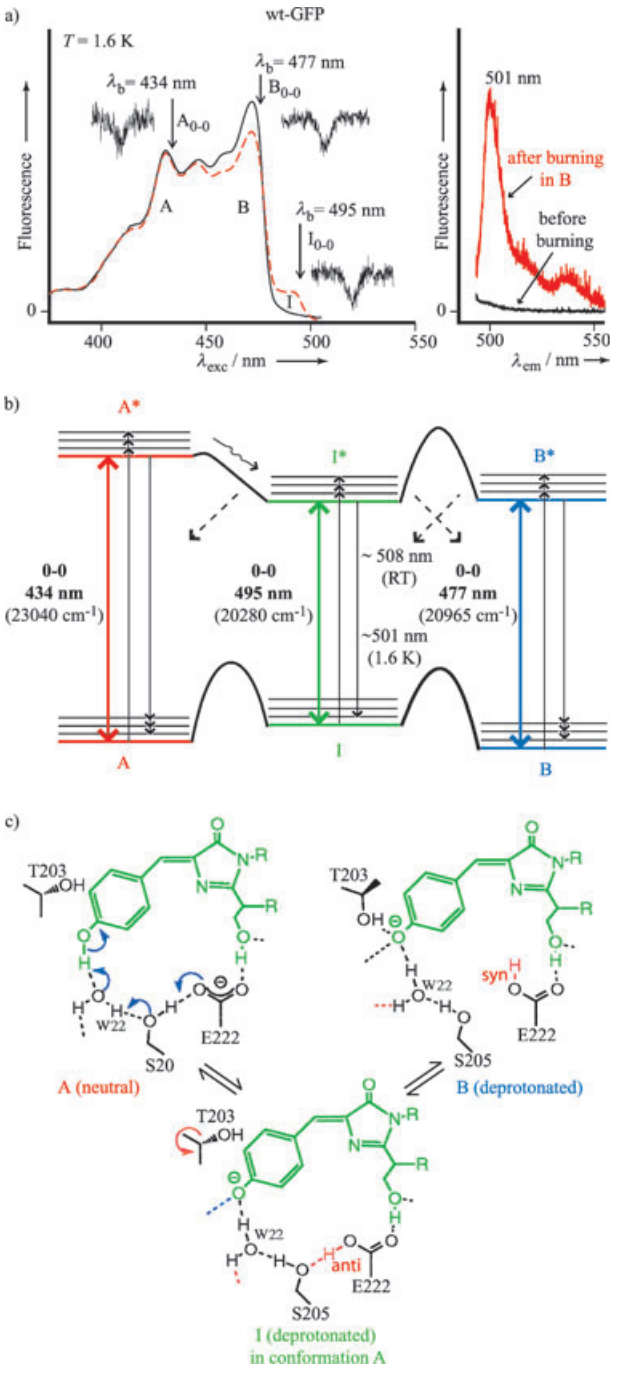

Figure 3. *wt-GFP. a) Left: Excitation spectrum at 1.6 K (detected at 510 nm) before (black) and after (red) irradiating the B form (at 450–480 nm), producing the I form. The 0–0 transitions of A, B and I were identified by hole burning. Insets: The holes in A, B and I are drawn on a wavelength scale different from that in the main figure at the positions of the arrows; their widths reflect the bandwidth of the laser of ≈1 cm^{-1}. Right: Emission spectra excited in the I form at ≈490 nm before (black) and after (red) burning in the B form. The photoinduced reaction is reversible.[37] b) Proposed energy-level diagram[37] of the three photoconvertible forms A, B and I. The 0–0 transitions are given. The dashed diagonal arrows indicate photoinduced radiationless conversions, probably via the triplet state. The only photoconversion observed in the excited state is that from A* to I*. The ground-state energy-level differences are of the order of a few hundred wavenumbers; the energy-barrier heights are a few thousand wavenumbers. At low temperatures further intermediate forms are present, which are not drawn for simplicity. c) Proposed structures of the chromophore and its direct hydrogen-bonding network in the A, I and B forms (based on refs. [31b, 35b]).*

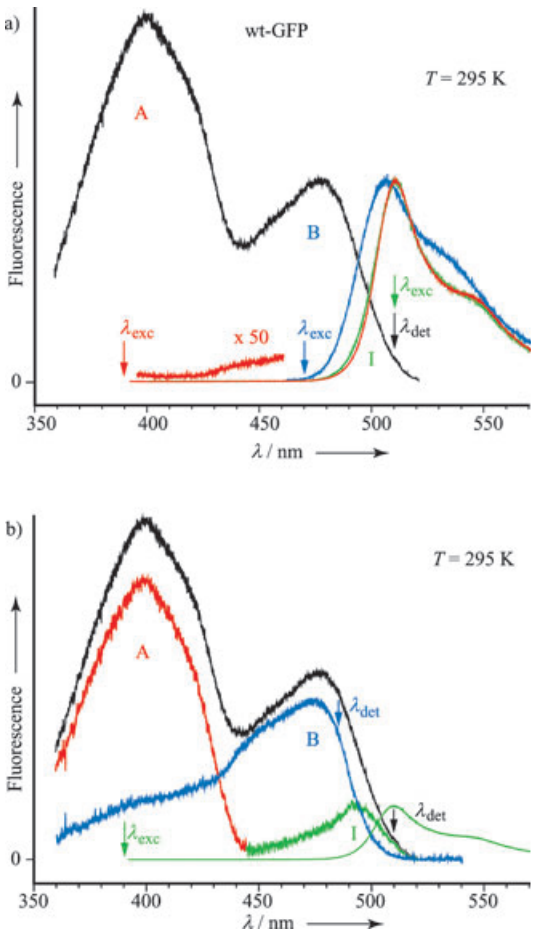

Figure 4. *wt-GFP. Wavelength-selective excitation and emission spectra at room temperature. Identification of the I form. a) Excitation spectrum detected at 510 nm (black) and emission spectra excited in the A form at 390 nm (red), the B form at 470 nm (blue) and the far-red wing at 510 nm (green). Excitation in the A form (red curve) yields a very weak emission from A* at wavelengths longer than ≈430 nm and the strong, characteristic green fluorescence with a maximum at ≈508 nm originating from I*. The emission spectrum excited in the B form (blue curve) is broader than that of I* with a maximum shifted to the blue by a few nanometers. Excitation in the far-red edge of the absorption spectrum (green curve) yields an emission spectrum identical to that excited in the A form (i.e., from I*). The intensities of the emission spectra have been normalized to the maximum of the excitation spectrum of the B form. b) Excitation spectra detected at 510 nm (black curve, A, B and I forms) and at 485 nm (blue curve, principally B form). The third excitation spectrum (red curve, A form and green curve, I form) is obtained after subtracting the two spectra from each other. The excitation and emission spectra of the I form (green curve) have approximate mirror symmetry.*

tion spectra of wt-GFP at 1.6 K before and after irradiation of the B form with ≈50–100 mWcm^{-2} for 30–60 min. A selective bleaching of the B form occurs with simultaneous emergence of a new band at ≈490–500 nm (red dashed line) that we have assigned to the I form. The emission spectrum obtained on excitation of this newly produced I band, the red solid curve at the right, is similar to that obtained on excitation of the A form (Figure 2b, dashed blue curve). Thus, a stable I form is produced in the ground state at 1.6 K through a radiationless conversion from B* to I, probably via the triplet state, because no emission from I* is observed when exciting B. This conclusion was derived from a series of emission spectra as a

function of λ_{exc} shown in Figure 3a of ref. [37] Inversely, when I is photobleached, it photoconverts by a radiationless process back from I* to B (not shown). When irradiating the A form with a laser at 400–430 nm, a similar stable photoproduct in the ≈500 nm region is found, most probably through the conversion A→A*→I*→I. On closer inspection, we have noticed that by irradiation of the A form, two weaker, additional I forms were produced at ≈500 nm and ≈510 nm. By studying the temperature dependence of the multiple I forms, we have found that only one of them remains populated at ambient temperature (see Section 3.2). "Extra" I forms produced by hole burning at low temperatures, and their variations with temperature, have also been reported in the literature for wt-GFP[58] and the isolated GFP chromophore in alcohol solutions.[42b]

By selective laser excitation, it was further discovered in ref. [37] that narrow holes could be burnt exclusively at the spectral positions of the 0–0 transitions within a range of a few nanometers determined by an inhomogeneous linewidth of a few hundred wavenumbers. Thus, the 0–0 transition of the A form was located around 434 nm, whereas those of the B and I forms around, respectively, 477 nm and 495 nm (Figure 3a, left). It should be remarked that the hole widths measured in these experiments are limited by the laser bandwidth of $\approx 1\ cm^{-1}$ and are not representative of the homogeneous linewidth (see Section 4.4). Burning into vibronic transitions yields much broader holes because vibronic bands decay much faster than 0–0 transitions (pico- versus nanosecond).[54] By measuring zero-phonon holes and their phonon-side holes, we could estimate the electron–phonon coupling strength for wt-GFP to be $S = 4.0 \pm 0.5$.[37] For the isolated GFP chromophore in solution it was speculated that it should have a much larger S value than wt-GFP because no narrow holes were recorded.[42b]

From the detailed results obtained by the combination of fluorescence line narrowing and hole burning, the photo-interconversion pathways of the A, I and B forms were established in an energy-level diagram.[37] Similar schemes have subsequently been proposed in our group for mutants of GFP,[38] differing only in the details. The results for wt-GFP are summarized in Figure 3b: the I form is not populated at 1.6 K in a fresh, unilluminated sample and is weakly populated at 295 K (see also Figure 4). Thus, the ground state of I must lie above that of B and A by a few hundred wavenumbers. The level scheme, as already mentioned, is somewhat more complicated than in Figure 3b because two more weakly absorbing I forms are photoinduced at low temperature. The energy-barrier heights between the ground states of the various forms, which we have recently determined from temperature-dependent experiments, are of the order of a few $1000\ cm^{-1}$, similar to those reported in ref. [58]. In the excited state, the barrier for the proton transfer process A*→I* proves to be low because only little emission is observed directly from A* at low temperature (Figure 2b, dashed blue curve) and almost none at room temperature (Figure 4a, red curve). The barrier for B*→I* should be at least $2000\ cm^{-1}$ because excitation into B* does not induce any measurable emission from I*, but it produces the I form in the ground state at low temperature. On burning I, that is, on prolonged I→I* irradiation, both the A and the B forms are recovered. The conversions B*→I, I*→B and I*→A, all seem to occur through radiationless processes.[37]

A proposed mechanism for the structures involved in the photoconversion of wt-GFP between the neutral A and the anionic B form of the chromophore (drawn in green in Figure 3c) is based on the X-ray data of wt-GFP[30] and the S65T mutant,[31b] molecular dynamics simulations[35b] and previous spectroscopic work.[40a,b] The change from A (upper left) to B (upper right) occurs in two, or even three,[35b] steps. The first one is a fast proton transfer (or "shuttle") reaction between the A* form and the I* form (lower middle). During this proton "shuttle", the glutamate-222 (E222) in the hydrogen-bonded network becomes protonated.[31b,c] The second step involves a conformational change (rotation) of the threonine 203 (T203) and a hydrogen-bond rearrangement between the deprotonated I and B forms. The precise path taken by a proton abstracted from the excited state of the chromophore is difficult to define due to the complexity of the hydrogen-bonding network.[3,35b]

In addition to wt-GFP, three red-shifted GFP-mutants (S65T, RS-GFP and EYFP) were studied in our laboratory.[38] These mutants were designed to absorb and emit light as photostable "one-color" proteins.[1,13–15] Our results, in contrast, have shown that these GFP mutants are not "one-color" systems because they can be reversibly phototransformed among at least three conformations (A, B and I) associated with the protonation state of the chromophore.[38] From the corresponding energy-level schemes we suggested, in ref. [38b], an explanation for the "on–off" and "blinking" behavior of specific single GFP-mutant molecules at room temperature.[48b,e] The reversible photo-interconversions seem to represent a more general phenomenon occurring also in other GFP mutants as well as in red fluorescent proteins.[52] This has important consequences for applications of GFP-mutants in the study of protein–protein interactions by FRET, where a change in the color of the fluorescence is commonly interpreted as a sign of energy transfer and, thus, for an interaction between different proteins. Such a color change may well arise from a photoinduced intramolecular conversion between various forms of a specific GFP mutant rather than from intermolecular processes between proteins[37,38] that one would like to study by FRET.

3.2. wt-GFP: Identification of the I form at Room Temperature

A first indication that the I form of wt-GFP is populated at 295 K but not at 1.6 K is given by the excitation and emission spectra at these two temperatures in Figure 2b (Section 3.1).[37] The spectra intersect at different wavelengths (≈500 nm at 295 K and 477 nm at 1.6 K), which would not occur if A and B were the only forms present in the ground state at room temperature. To confirm that the red wing in the excitation spectrum at 295 K indeed results from population of the I form in the ground state, we have taken systematically a series of excitation (and emission spectra) detected (and excited) every few

nanometers. Figure 4a, which represents one of such spectra, shows an excitation spectrum (black curve) together with three emission spectra excited in the maximum of the A form (red curve), the B form (blue curve) and in the far-red wing of the excitation spectrum (green curve). Remarkably, the spectrum drawn in red in Figure 4a with its maximum at ≈508 nm, representing the emission from I*, completely overlaps with that drawn in green. In contrast, the blue-colored spectrum, which corresponds to the emission from B*, is significantly broader, has a somewhat different shape and its maximum is at ≈503 nm. We conclude from these spectra that the I form is populated at room temperature and that it absorbs at the far-red wing of the excitation spectrum (≈500 nm). This finding is supported by the spectrum of the low-temperature photoproduct which we discovered (Section 3.2 and Figure 3a).[37]

We have also unravelled the shape and position of the excitation spectrum of the hidden I form (see Figure 4b). After recording two excitation spectra, one representing the (A+B+I) forms (black curve, detected at the maximum of the emission of the I form), and the other representing the B form (blue curve, detected at the blue edge of the emission spectrum of the B form), we subtracted the two spectra from each other to obtain the (A+I) forms. The amount of B subtracted from (A+B+I) was done in such a way that the shape (of the red part at ≈450–510 nm) of the difference spectrum (A+I) would resemble as much as possible the mirror image of the emission spectrum of the I form. We have verified that the shape and position of the resulting excitation spectrum of the I form is indeed independent of the detection wavelength of the (A+B+I) spectrum. The shape and position of the I spectrum shown in Figure 4b is further corroborated by the recently published spectrum of a GFP mutant which stabilizes the I form only.[59] From the variation of the fluorescence intensity as a function of temperature we have estimated the ground-state energy-level differences and energy-barrier heights between the A, B and I forms of wt-GFP (to be published).

4. DsRed and Other Red Fluorescent Proteins

The discovery of red fluorescent proteins (RFPs) from non-bioluminescent reef corals[24] caused a breakthrough because of their potential for multicolor protein-tracking applications and construction of improved FRET-pairs.[7,8a,25–29] In comparison to GFPs, the wavelength of the first absorption band of RFPs has a deeper tissue penetration and the emission is better separated from cellular autofluorescence. The so-called DsRed, which was the first cloned RFP, has a strong emission at 583 nm, a high quantum yield of ≈0.7 and its spectra are independent of the pH value between 5 and 12.[27a] But its use has severely been limited by a number of problems: slow and incomplete maturation and tetramerization (even at nanomolar concentrations).[7,25,27,28,48e,f,60–62] The incomplete maturation, even after 30 h at 37 °C, involves an intermediate step in which an "immature" green (G) emitting species is irreversibly transformed into the red (R) emitting species.[27] The tetramerization is responsible for energy transfer (ET) from the G to the R species within the DsRed protein. Evidence for G-to-R energy transfer derives from photobleaching,[27] fluorescence anisotropy and depolarization,[60] picosecond time-resolved fluorescence[61] and SM experiments.[48e,f,62] The tetramerization problem has been solved by a combination of targeted and random mutagenesis (33 mutations), yielding a monomeric DsRed variant called mRFP1.[29] Recently, a number of new red fluorescent proteins and nonfluorescent chromoproteins (CPs) have been discovered and cloned, some of them with fast maturation and others with emission peaks up to 649 nm, but only a few RFPs have been minimally characterized.[7,25,34a,b,c]

4.1. Reversible Photoconversions and "Downhill" Energy Transfer in DsRed at Low Temperatures

To get a better understanding of the intricate photophysics of red fluorescent proteins, complicated by their tetramerization and incomplete maturation, we carried out a high-resolution optical spectroscopy study of DsRed at 1.6 K and as a function of temperature up to 295 K. The structure of DsRed[32] is similar to that of GFPs and consists of a 28 kDa "β-barrel" protein with 225 amino acid residues. Its "β-barrels", however, are oligomerized into tetramers (Figure 5a, left inset). The large spectral red-shift of ≈80 nm with respect to wt-GFP arises from two additional conjugated double bonds C=N–C=O in the chromophore, which are responsible for the extended π–π electron system (Figure 5a, right inset).

The excitation spectrum of a previously unilluminated DsRed sample at 1.6 K (Figure 5a, black) shows a maximum at 555 nm and two well-defined bands at ≈514 and 480 nm. The first two features correspond to the origin and a vibronic band of the mature red (R) form. The feature at 480 nm contains a contribution from the "immature" green (G-) form. Although DsRed is more photostable than GFPs,[27] we have discovered that it undergoes reversible photoconversions between various forms at low temperatures, in addition to "downhill" energy transfer (ET) within its tetrameric structure.[52] The excitation spectrum after irradiation ("burning") of the R form at 514 nm, shown in blue, illustrates this. While the bands belonging to R decrease in intensity, two new bands appear at $\lambda_{exc} < 480$ nm and at $\lambda_{exc} > 560$ nm. We have called the photoproduct to the red side of the R form, the shifted-red (SR) form and that towards the blue side, the green (G′) form. The latter absorbs in the same spectral region as the G form. The $S_1 \leftarrow S_0$ 0–0 transitions of the R, SR and G forms were identified by hole burning in a similar way as described in Section 3.1 for GFPs.[37,38] The "immature" G form proved to be photostable and no holes could be burnt into it. From the intersection of the excitation and emission spectra of the G form, we have estimated its 0–0 transition at 484 nm.[52] The holes of the SR, R and G′forms are shown in Figure 5b at the left.

In Figure 5b at the right, a series of fluorescence spectra for three different excitation wavelengths are reproduced, before (black) and after irradiation of the R form at 514 nm with ≈200 mWcm^{-2} for 30 minutes (dashed), 60 minutes (dotted) and 90 minutes (solid grey). The spectra in the middle of Figure 5b show the red fluorescence of the R form before irradia-

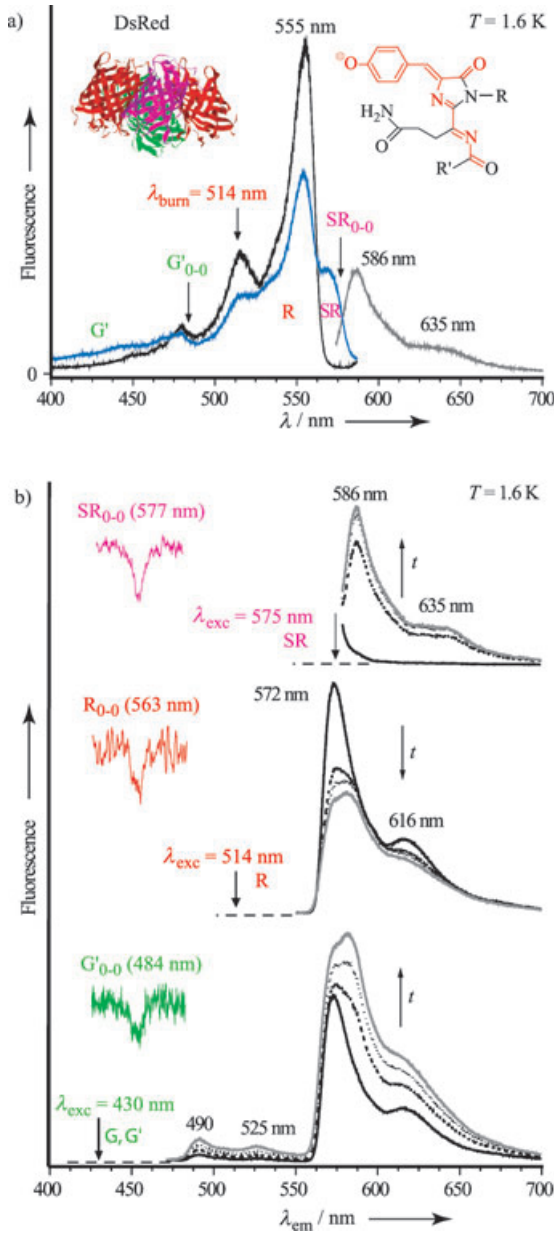

Figure 5. *DsRed. a) Excitation spectra at 1.6 K detected at 590 nm before (black curve) and after (blue curve) irradiation of the red (R) form with an argon ion laser at 514 nm with ≈200 mW cm^{-2} for 90 min, together with an emission spectrum of the photoinduced SR form (grey) excited with ≈1–5 mW cm^{-2} at ≈575 nm. Inset, left: tetrameric β-barrel crystal structure. An example has been chosen with a tetramer containing two R, one G and one SR subunit. Inset, right: chromophore. b) Left (from top to bottom): Holes burnt for about 15 min with ≈2–5 mW cm^{-2} into the 0–0 transition of the SR form at ≈577 nm, the R form at ≈563 nm and the G′ form at ≈484 nm. The widths of the holes are limited by the laser bandwidth of ≈1 cm^{-1}.[52] Right: Emission spectra before (solid black) and after irradiation of the R form with ≈200 mW cm^{-2} for 30 min (dashed), 60 min (dotted) and 90 min (solid grey). Top: excitation of the SR form at 575 nm. Middle: excitation of the R form at 514 nm. Bottom: excitation of the G and G′ forms at 430 nm.*

tion (black curve) and on progressive irradiation of the R form. The emission spectrum not only decreases, but also broadens and slightly shifts towards the red. We attribute the decrease in fluorescence intensity to a decrease of the number of R subunits within the tetramers due to photoconversion. The broadening and shift we have attributed to "downhill" energy transfer from R to SR (see below). With λ_{exc} = 575 nm (top of Figure 5b) the emission originates from the photoinduced SR form which is shifted 14 nm to the red from that of the R form. Its intensity increases as a function of irradiation time and its shape is approximately mirror symmetric with respect to the SR excitation spectrum (Figure 5a). Because the shape of the emission spectrum is similar to that of the R form (Figure 5b, middle) and its position is only ≈430 cm^{-1} (14 nm) shifted to the red of the latter, we think that SR is chemically similar to R, differing only in its conformational arrangement within the surrounding hydrogen-bonding network. It is conceivable that the SR form is related to the deprotonated R form in a similar way as the I and B forms are related in GFPs.[37,38]

The bottom spectra in Figure 5b are emission spectra excited at 430 nm at which wavelength, in a previously unilluminated sample, only the "immature" green (G) form absorbs. The emission spectrum before irradiation in R (black curve) consists of two regions: a weak emission between ≈490 and 550 nm arising from the directly excited "immature" green (G) form, and a strong emission between 570 and 700 nm that originates from the indirectly excited R form. We ascribe this strong, red emission to "downhill" energy transfer (ET) from the excited G form (donor) to the R form (acceptor) within a tetramer of DsRed. Since the number of subunits in the R form decreases as a function of irradiation time, while that in the SR and G′ forms increases, we expect the emission in the green region to increase with time, as indeed observed. We should remark that the emission of G′ builds up on top of that of G (grey curves), but with a slightly different shape. To our surprise, we noticed that the emission spectrum in the red region also increases on irradiation of the R form, simultaneously changing its shape (Figure 5b, bottom). We interpret these changes in terms of "downhill" ET from the donors G and G′ to the acceptors R and SR within the DsRed tetramer. The change in shape and the shift to the red of the strong emission (grey curves) is most probably due to an increase of the number of SR subunit acceptors during the irradiation of R.

We have proven in ref. [52] that the results presented in Figure 5b are indeed a manifestation of "downhill" ET within the DsRed tetramer, because they fulfil the conditions related to Förster's mechanism based on nonradiative dipole–dipole interactions.[63] Further, the photoinduced conformational changes we have observed are reversible: the R form is recovered after irradiation of the photoproducts at 430 nm (G′) and 575 nm (SR). Thus, DsRed acts as an optical switch at 1.6 K (see also Figure 7).

4.2. Thermally Induced Conformational Changes in DsRed

The relative energies of the ground states of the R, SR and G′ forms of DsRed and the heights of the barriers between them were obtained from a series of spectra taken between 1.6 K and room temperature.[52] Figure 6a shows emission spectra as a function of temperature of the SR form (grey curves 1–4) on excitation at 575 nm after irradiation of the

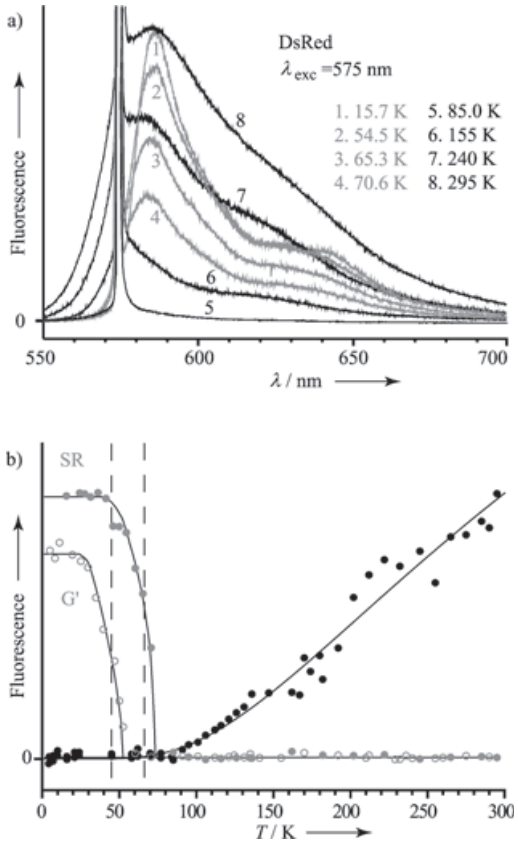

Figure 6. *DsRed. a) Emission spectra of the SR form as a function of temperature excited at 575 nm (grey curves 1–4). Prior to this experiment SR had been photoproduced at 1.6 K by irradiation of the R form at 514 nm with* $\approx$*200 mW cm*$^{-2}$ *for* $\approx$*1 hour. The strong signal at 575 nm is caused by laser scattering from the sample. The fluorescence intensity of the SR form decreases with increasing temperature and disappears at* $\approx$*80 K. The increase of fluorescence intensity above* $\approx$*90 K (black curves 6–8) is attributed to emission from the R form excited at 575 nm in a "hot band" of R. b) Fluorescence intensity of the SR form at 586 nm (grey solid dots) excited at 575 nm and of the G′ form at 525 nm (grey open dots) excited at 430 nm, after having both species been photoproduced at 1.6 K (see Figure 6a), as a function of temperature. The emission intensities of both forms remain constant until the intensity of G′ drops at* $\approx$*45 K and that of SR at* $\approx$*65 K. Neither form reappears up to room temperature. The black solid dots show the increase of the fluorescence intensity of the R form at* $T > 90$ *K (the curve is a guide to the eye) caused by excitation of the "hot band" at 575 nm. The black solid dots plotted between 0 and 80 K were also measured on excitation at 575 nm in a previously nonirradiated sample where SR is absent.*

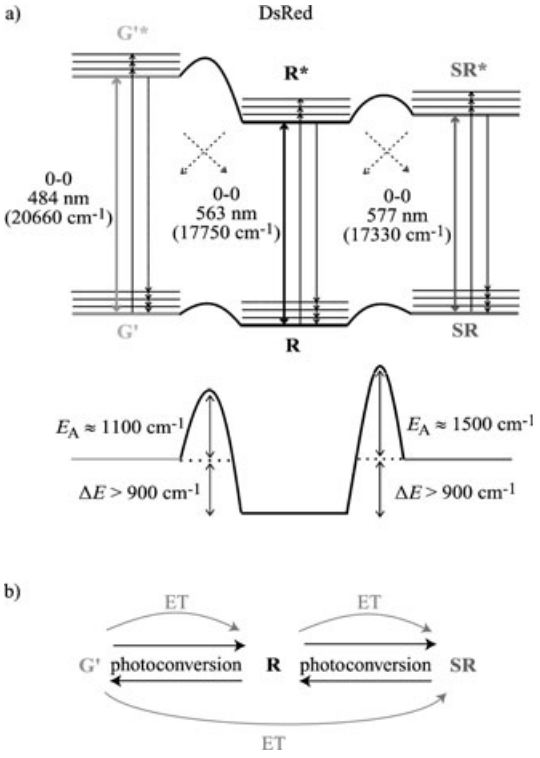

Figure 7. *DsRed. a) Energy-level diagram of the three photoreversible forms. The 0–0 transitions of the "mature" R form and the photoinduced SR and G′ forms are shown. The relative ground-state energy levels and energy-barrier heights between the three forms, determined from temperature-dependent spectra, are indicated in the lower part. b) Summary of the reversible photoconversions at low temperatures and the "downhill" energy-transfer (ET) pathways.*[52]

R form at at 514 nm 1.6 K. The fluorescence intensity of SR decreases with increasing temperature and vanishes at $\approx$80 K (see also Figure 6b, grey filled circles). Between 85 and 295 K, a new spectrum grows in, which shifts to the red and is much broader than that of the SR form (black curves 5–8). Because this spectrum appears only at $T = 90$ K and its shape is identical to that of the emission spectrum of the R form (excited at 514 nm) at the corresponding temperature, we attribute it to the emission of the R form on excitation into a "hot band" at 575 nm, that is, a transition that is excited from a thermally populated vibration of the ground state of R to the first electronic state.

In the experiments shown in Figure 6b (solid and open dots), the R form was first irradiated at 514 nm at 1.6 K, and the SR and G′ forms were photoproduced. Subsequently, the intensities of the maximum of the fluorescence of the SR form (grey solid dots) at 586 nm, the G′ form (grey open dot) at 525 nm and the R form (black solid dots) at 580 nm, excited in a "hot band" at 575 nm, were followed while the temperature of the sample gradually increased. The SR form was found to be thermally stable up to $\approx$60 K; at $\approx$65 K its fluorescence rapidly decreased. Similarly, the intensity of the G′ form rapidly decreased at $\approx$45 K. None of these forms reappeared (within the error bars) at higher temperatures. In contrast, the emission of the R form only appears at $T > 90$ K due to excitation in a "hot band" of R. The black solid dots between 0 and 80 K were obtained on excitation at 575 nm in a sample where SR had not been previously photoinduced. We have interpreted the behavior of the SR and G′ forms in terms of an Arrhenius-activated process with energy barriers E_A between SR and R, and between G′ and R (see Figure 7a), and a rate k to cross-over the barrier, $k = k_A \exp(-E_A/k_bT)$. The rate of disappearance of the emission of the SR and G′ forms was $\approx$(10–30 min)$^{-1}$ at about 65 and 45 K, respectively. Assuming a pre-exponential factor $k_A \approx 10^{11}$–10^{12} s^{-1}, we have estimated the following barrier heights: $E_A \approx 1500$ cm$^{-1} \pm 100$ cm^{-1} between SR and R, and $E_A \approx 1100$ cm$^{-1} \pm 100$ cm^{-1} between G′ and R (Figure 7a, bottom). Since neither SR nor G′ reappears up to room temperature (295 K), the energy difference ΔE between the

ground states of G′ and R, and between SR and R, must be at least $\Delta E > 900\ cm^{-1}$ (Figure 7a, bottom). We have observed that the fluorescence of the R form on excitation of the "hot band" only appears gradually above $T \approx 90$ K (Figure 6b, black solid dots). Assuming that Boltzmann equilibrium has been established between the ground state and the "hot" vibrational state of the R form at $T > 90$ K, that is, $I_{hot}/I_R \approx \exp(-\Delta E/k_bT) \approx 0.01$ at 90 K, we have estimated the energy difference between these two states to be $\Delta E \approx 250$–$300\ cm^{-1}$. To shed light on the energy landscapes in the ground and excited state of DsRed, we have developed a model to simulate the shapes of the spectral bands and their broadenings and shifts as a function of temperature (to be published).

Figure 7 contains the summary of the above-mentioned results for DsRed. The top diagram shows the $S_1 \leftarrow S_0$ 0–0 transitions of the R, SR and G′ forms identified by spectral hole burning at 1.6 K and the energy-barrier heights and energy differences between these forms in their ground states. The 0–0 transition of the G form was estimated to be at 484 nm;[52] because of its photostability the ground-state energy of G relative to that of the other forms is unknown. Although we do not know what the nature of the G′ species is, we envisage two possibilities: 1) On irradiation of the R form, the path of conjugation of the electronic π–π* system might be interrupted by the addition of water to the C=N bond, in a similar way as proposed for a mildly denatured form of DsRed.[27b] 2) By analogy with wt-GFP,[37] G′ might be the result of protonation of R. Whatever G′ is, one has to take into account that it can be photoinduced back to the R form.

The reversible photoconversions and "downhill" energy-transfer (ET) processes that take place are sketched in Figure 7b. These photoconversions might be detrimental in experiments whenever DsRed is used for multi-color tracking because its color can change under illumination. Also "intra-tetramer" ET from G and/or G′ to R and SR might become a problem when using GFP as donor together with DsRed as acceptor in FRET experiments. At room temperature we have observed additional irreversible processes when irradiating the R form at 514 nm with rather high power (a few $W\,cm^{-2}$) for a prolonged period of time (a few hours).[52] Similar irreversible photoconversions in DsRed under strong irradiation have been reported in the literature.[51b,48f]

4.3. Homogeneous Linewidth and Optical Dephasing in DsRed

To get insight into the dynamic interactions between the chromophore and its surrounding protein, we have investigated the optical dephasing of DsRed at low temperature. In comparison to other pigment–protein complexes where the chromophore is extrinsically or noncovalently bound to the protein, the chromophore forms part of the protein backbone and is rigidly held in a hydrogen-bonding network in autofluorescent proteins. We succeeded in determining the unknown "effective" homogeneous linewidth Γ'_{hom} of the $S_1 \leftarrow S_0$ 0–0 transition of the R form of DsRed as a function of temperature between 1.2 and 4.2 K by means of megahertz-resolution hole burning.[53] Holes were burnt with a 2 MHz-bandwidth continuous wave (cw) dye laser in the red wing of the absorption band (between 565 and 568 nm, see Figure 8b) and Γ_{hom} was obtained[54] by extrapolating the width of the holes Γ_{hole} to zero burning-fluence density $Pt/A \rightarrow 0$ (where P is the power of the laser, t the burning time and A the area of the laser spot on the sample). At 1.2 K, $\Gamma'_{hom} \approx 1$ GHz (see Figure 8a), a value similar to those previously reported for doped organic glasses[54,6] and photosynthetic systems.[54c,56,64b] The data in Figure 8a follow the well-known $T^{1.3\pm0.1}$ temperature dependence[54] and extrapolate to $\Gamma_0 = (2\pi\tau_{fl})^{-1} \approx 50$ MHz for $T \rightarrow 0$, with $\tau_{fl} \approx 3.5$ ns, the fluorescence lifetime of DsRed.[61] This implies that energy transfer (ET) does not take place between the DsRed molecules excited in the far-red wing of the spectrum. If ET would occur on a 10-ps time scale as reported at room temperature,[61] this would be reflect in a Γ_0 value in excess of 15 GHz ($= 0.5\ cm^{-1}$). The $T^{1.3}$ power law, also observed for organic glassy systems[54a,b,64a] and a few biological complex-

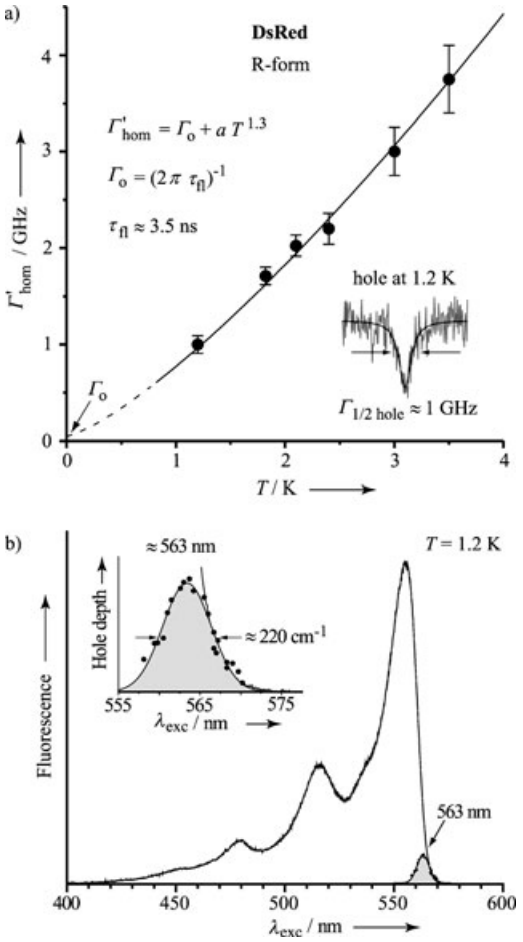

Figure 8. *DsRed. a) "Effective" homogeneous linewidth Γ'_{hom} of the R form (excited in the red wing of the 0–0 band at 567 nm) as a function of temperature T. Γ'_{hom} follows a $T^{1.3}$ power law and extrapolates to the fluorescence lifetime-limited value $\Gamma_0 \approx 50$ MHz, with $\tau_{fl} \approx 3.5$ ns.[61] Inset: hole at 1.2 K yielding Γ'_{hom}. b) Excitation spectrum of DsRed at 1.6 K (as in Figure 5a) showing the spectral distribution of "traps" in the red wing. No energy transfer occurs on excitation of molecules in these "traps". Inset: amplified plot of the "trap" distribution obtained from the hole depth versus excitation wavelength (of holes having equal width and burnt with low fluence).[53]*

es,[54c,64b] suggests that two-level systems (TLSs)[54] are responsible for the dephasing.

In addition to hole widths, we have also measured hole depths as a function of excitation wavelength (see Figure 8b, inset) from which we have obtained the spectral distribution of "traps", that is, of molecules that do not undergo intramolecular "downhill" ET. This distribution has a width of $\approx 220\ cm^{-1}$ and a relative area that is less than 10% of that of the excitation spectrum of the R form, indicating that the majority of the molecules in the absorption band of DsRed are involved in energy transfer, in agreement with its tetrameric structure.[53]

Finally, using the hole-burning model of ref. [65] we have estimated the electron–phonon coupling strength S of the red (R) form of DsRed to be $S = 3.5 \pm 0.25$, a value that is comparable to that of wt-GFP ($S \sim 4.0 \pm 0.5$).[37] This value is much larger than that of, for example, the photosystem II reaction center of green plants ($S = 0.76$).[56] We interpret this rather strong electron–phonon coupling, which appears to be correlated with the coupling constant a of the dephasing equation (Figure 8a), as a reflection of the tight binding of the chromophore to the hydrogen-bonded network.[53]

5. Summary and Outlook

In this Minireview we have demonstrated that the combination of hole burning and site-selective laser excitation and emission spectroscopy at low temperatures with variable-temperature experiments sheds new light on the photodynamics of autofluorescent proteins. We have shown how to 1) disentangle photoconvertible forms, 2) identify 0–0 transitions, 3) determine pathways of photo-interconversion, 4) prove the existence of "downhill" energy transfer, 5) obtain energy-barrier heights and energy-level differences between conformations, 6) determine the homogeneous linewidth and its temperature dependence, 7) obtain spectral distributions of "trap" molecules and 8) estimate electron–phonon coupling strengths.

There is a continuous development of new fluorescent proteins in order to extend their wavelength range and to improve their brightness and photostability. With site-selective spectroscopic techniques as used here, in combination with single-molecule detection, it should be feasible to study the properties and mechanisms of far-red fluorescent monomeric photoactivatable proteins. Controllable changes of color are within reach, and *in vivo* optical switches are becoming a reality.[7,8,18–20,25,34]

Acknowledgements

We would like to thank J. H. van der Waals (Leiden) for his continuous support and critical comments, and R. J. Silbey (MIT, USA) for exciting discussions on models and simulations. The samples were a kind gift of V. Subramaniam and T. M. Jovin, Max-Planck Institute for Biophysical Chemistry, Göttingen. This work was financially supported by the Netherlands Foundation for Physical Research (FOM) and the Council for Chemical Research of the Netherlands Organization for Scientific Research (NWO-CW).

Keywords: energy transfer · fluorescence spectroscopy · laser spectroscopy · photochemistry · proteins

[1] R. Y. Tsien, *Annu. Rev. Biochem.* **1998**, *67*, 510–544, and references therein.
[2] *Green Fluorescent Protein: Properties, Applications and Protocols* (Eds.: M. Chalfie, S. Kain), Wiley, New York, **1998**.
[3] F. G. Prendergast, *Methods Cell Biol.* **1999**, *58*, 1–18.
[4] *Green Fluorescent Proteins* (Eds.: K. Sullivan, S. Kay), Academic Press, San Diego, **1999**.
[5] J. Lippincott-Schwartz, E. Snapp, A. Kenworthy, *Nat. Rev. Mol. Cell Biol.* **2001**, *2*, 444–456, and references therein.
[6] M. Zimmer, *Chem. Rev.* **2002**, *102*, 759–781, and references therein.
[7] J. Zhang, R. E. Campbell, A. Y. Ting, R. Y. Tsien, *Nat. Rev. Mol. Cell Biol.* **2002**, *3*, 906–918, and references therein.
[8] a) J. Lippincott-Schwartz, G. H. Patterson, *Science* **2003**, *300*, 87–91, and references therein; b) G. H. Patterson, J. Lippincott-Schwartz, *Methods* **2004**, *32*, 445–450.
[9] D. C. Prasher, V. K. Eckenrode, W. W. Ward, F. G. Prendergast, M. J. Cormier, *Gene* **1992**, *111*, 229–233.
[10] a) M. Chalfie, Y. Tu, G. Euskirchen, W. W. Ward, D. C. Prasher, *Science* **1994**, *263*, 802–805; b) H. Yokoe, T. Meyer, *Nat. Biotechnol.* **1996**, *14*, 1252–1256.
[11] C. W. Cody, D. C. Prasher, W. M. Westler, F. G. Prendergast, W. W. Ward, *Biochemistry* **1993**, *32*, 1212–1218.
[12] R. Heim, D. C. Prasher, R. Y. Tsien, *Proc. Natl. Acad. Sci. USA* **1994**, *91*, 12501–12504.
[13] A. B. Cubitt, R. Heim, S. R. Adams, A. E. Boyd, L. A. Gross, R. Y. Tsien, *Trends Biochem. Sci.* **1995**, *20*, 448–455.
[14] a) R. Heim, A. B. Cubitt, R. Y. Tsien, *Nature* **1995**, *373*, 663–664; b) M. Ormö, A. B. Cubitt, K. Kallio, L. A. Gross, R. Y. Tsien, S. J. Remington, *Science* **1996**, *273*, 1392–1395.
[15] R. Heim, R. Y. Tsien, *Curr. Biol.* **1996**, *16*, 178–182.
[16] G. H. Patterson, S. M. Knobel, W. D. Sharif, S. R. Kain, D. W. Piston, *Biophys. J.* **1997**, *73*, 2782–2790.
[17] a) T. B. McAnaney, E. S. Park, G. T. Hanson, S. J. Remington, S. G. Boxer, *Biochemistry* **2002**, *41*, 15489–15494, and references therein; b) O. Griesbeck, G. S. Baird, R. E. Campbell, D. A. Zacharias, R. Y. Tsien, *J. Biol. Chem.* **2001**, *276*, 29188–29194.
[18] G. H. Patterson, J. Lippincott-Schwartz, *Science* **2002**, *297*, 1873–1877.
[19] R. Ando, H. Hama, M. Yamamoto-Hino, H. Mizuno, A. Miyawaki, *Proc. Natl. Acad. Sci. USA* **2002**, *99*, 12651–12656.
[20] D. M. Chudakov, V. V. Belousov, A. G. Zaraisky, V. V. Novoselov, D. B. Staroverov, D. B. Zorov, S. Lukyanov, K. A. Lukyanov, *Nat. Biotechnol.* **2003**, *21*, 191–194.
[21] a) A. Miyawaki, *Current Op. Neurobiol.* **2003**, *13*, 591–596; b) A. Miyawaki, *Developmental Cell* **2003**, *4*, 295–305, and references therein.
[22] D. A. Zacharias, G. S. Baird, R. Y. Tsien, *Current Opinion Neurobiol.* **2000**, *10*, 416–421.
[23] a) R. M. Hoffman, *Lancet Oncol.* **2002**, *3*, 546–556; b) R. M. Hoffman, *Acta Histochem.* **2004**, *106*, 77–82.
[24] M. V. Matz, A. F. Fradkov, Y. A. Labas, A. P. Savitsky, A. G. Zaraisky, M. L. Markelov, S. A. Lukyanov, *Nat. Biotechnol.* **1999**, *17*, 969–973.
[25] V. V. Verkhusha, K. A. Lukyanov, *Nat. Biotechnol.* **2004**, *22*, 289–295, and references therein.
[26] H. Mizuno, A. Sawano, P. Eli, H. Hama, A. Miyawaki, *Biochemistry* **2001**, *40*, 2502–2510.
[27] a) G. S. Baird, D. A. Zacharias, R. Y. Tsien, *Proc. Natl. Acad. Sci. USA* **2000**, *97*, 11984–11989; b) L. A. Gross, G. S. Baird, R. C. Hoffman, K. K. Baldridge, R. Y. Tsien, *Proc. Natl. Acad. Sci. USA* **2000**, *97*, 11990–11995.
[28] a) B. J. Bevis, B. S. Glick, *Nat. Biotechnol.* **2002**, *20*, 83–87; b) J. Wiedermann, A. Schenk, C. Röcker, A. Girod, K. D. Spindler, G. U. Nienhaus, *Proc. Natl. Acad. Sci. USA* **2002**, *99*, 11646–11651.
[29] R. E. Campbell, O. Tour, A. E. Palmer, P. A. Steinbach, G. S. Baird, D. A. Zacharias, R. Y. Tsien, *Proc. Natl. Acad. Sci. USA* **2002**, *99*, 7877–7882.
[30] F. Yang, L. G. Moss, G. N. Phillips, *Nat. Biotechnol.* **1996**, *14*, 1246–1251.

[31] a) R. M. Wachter, B. A. King, R. Heim, K. Kallio, R. Y. Tsien, S. G. Boxer, S. J. Remington, *Biochemistry* **1997**, *36*, 9759 – 9765; b) K. Brejc, T. K. Sixma, P. A. Kitts, S. R. Kain, R. Y. Tsien, M. Ormö, S. J. Remington, *Proc. Natl. Acad. Sci. USA* **1997**, *94*, 2306 – 2311; c) G. J. Palm, A. Zdanov, G. A. Gaitanaris, R. Stauber, G. N. Pavlakis, A. Wlodawer, *Nat. Struct. Biol.* **1997**, *4*, 361 – 365; d) R. M. Wachter, M.-A. Elsliger, K. Kallio, G. T. Hanson, S. J. Remington, *Structure* **1998**, *6*, 1267 – 1277; e) R. Battistutta, A. Negro, G. Zanotti, *Proteins* **2000**, *41*, 429 – 437.

[32] a) M. A. Wall, M. Socolich, R. Ranganathan, *Nat. Struct. Biol.* **2000**, *7*, 1133 – 1138; b) D. Yarbrough, R. M. Wachter, K. Kallio, M. V. Matz, S. J. Remington, *Proc. Natl. Acad. Sci. USA* **2001**, *98*, 462 – 467.

[33] a) M. Prescott, M. Ling, T. Beddoe, A. J. Oakley, S. Dove, O. Hoegh-Guldberg, R. J. Devenish, J. Rossjohn, *Structure* **2003**, *11*, 275 – 284; b) J. Petersen, P. G. Wilmann, T. Beddoe, A. J. Oakley, R. J. Devenish, M. Prescott, J. Rossjohn, *J. Biol. Chem.* **2003**, *278*, 44626 – 44631.

[34] a) G. H. Patterson, *Nat. Biotechnol.* **2004**, *22*, 1524 – 1525; b) N. C. Shaner, R. E. Campbell, P. A. Steinbach, B. N. G. Giepmans, A. E. Palmer, R. Y. Tsien, *Nat. Biotechnol.* **2004**, *22*, 1567 – 1572; L. Wang, W. C. Jackson, P. A. Steinbach, R. Y. Tsien, *Proc. Natl. Acad. Sci. USA* **2004**, *101*, 16745 – 16749.

[35] a) V. Helms, *Current Op. Struct. Biol.* **2002**, *12*, 169 – 175, and references therein; b) M. A. Lill, V. Helms, *Proc. Natl. Acad. Sci. USA* **2002**, *99*, 2778 – 2781, and references therein.

[36] A. A. Voityuk, A. D. Kummer, M. E. Michel-Beyerle, N. Rösch, *Chem. Phys.* **2001**, *269*, 83 – 91, and references therein.

[37] T. M. H. Creemers, A. J. Lock, V. Subramaniam, T. M. Jovin, S. Völker, *Nat. Struct. Biol.* **1999**, *6*, 557 – 560.

[38] a) T. M. H. Creemers, A. J. Lock, V. Subramaniam, T. M. Jovin, S. Völker, *Proc. Natl. Acad. Sci. USA* **2000**, *97*, 2974 – 2978; b) T. M. H. Creemers, A. J. Lock, V. Subramaniam, T. M. Jovin, S. Völker, *Chem. Phys.* **2002**, *275*, 109 – 121.

[39] a) M. E. Martin, F. Negri, M. Olivucci, *J. Am. Chem. Soc.* **2004**, *126*, 5452 – 5464; b) T. Laino, R. Nifosi, V. Tozzini, *Chem. Phys.* **2004**, *298*, 17 – 28, and references therein.

[40] a) M. Chattoraj, B. A. King, G. U. Bublitz, S. G. Boxer, *Proc. Natl. Acad. Sci. USA* **1996**, *93*, 8362 – 8367; b) H. Lossau, A. Kummer, R. Heinecke, F. Pöllinger-Dammer, C. Kompa, G. Bieser, T. Jonsson, C. M. Silva, M. M. Yang, D. C. Youvan, M. E. Michel-Beyerle, *Chem. Phys.* **1996**, *213*, 1 – 16; c) A. D. Kummer, J. Wiehler, T. Schüttrigkeit, B. W. Berger, B. Steipe, M. E. Michel-Beyerle, *ChemBioChem* **2002**, *3*, 659 – 663, and references therein; d) K. Winkler, J. Lindner, V. Subramaniam, T. M. Jovin, P. Vöhringer, *Phys. Chem. Chem. Phys.* **2002**, *4*, 1072 – 1081; e) J. T. M. Kennis, D. S. Larsen, I. H. M. van Stokkum, M. Vengris, J. J. van Thor, R. van Grondelle, *Proc. Natl. Acad. Sci. USA* **2004**, *101*, 17988 – 17993.

[41] a) D. Mandal, T. Tahara, S. R. Meech, *J. Phys. Chem. B* **2004**, *108*, 1102 – 1107, and references therein; b) M. Vengris, I. H. M. van Stokkum, X. He, A. F. Bell, P. J. Tonge, R. van Grondelle, D. S. Larsen, *J. Phys. Chem. A.* **2004**, *108*, 4587 – 4598, and references therein; c) P. Didier, L. Guidoni, G. Schwalbach, M. Bourotte, A. Follenius-Wund, C. Pigault, J.-Y. Bigot, *Chem. Phys. Lett.* **2002**, *364*, 503 – 510; d) A. D. Kummer, C. Kompa, H. Niwa, T. Hirano, S. Kojima, M. E. Michel-Beyerle, *J. Phys. Chem. B* **2002**, *106*, 7554 – 7559, and references therein.

[42] a) H. Niwa, S. Inouye, T. Hirano, T. Matsuno, S. Kojima, M. Kubota, M. Ohashi, F. I. Tsuji, *Proc. Natl. Acad. Sci. USA* **1996**, *93*, 13617 – 13622; b) M. Stübner, P. Schellenberg, *J. Phys. Chem. A* **2003**, *107*, 1246 – 1252.

[43] L. H. Andersen, H. Bluhme, S. Boyé, T. J. D. Jørgensen. H. Krogh, I. B. Nielsen, S. Brønsted Nielsen, A. Svendsen, *Phys. Chem. Chem. Phys.*, **2004**, *6*, 2617 – 2627, and references therein.

[44] a) M. H. J. Seifert, D. Ksiazek, M. K. Azim, P. Smialowski, N. Budisa, T. A. Holak, *J. Am. Chem. Soc.* **2002**, *124*, 7932 – 7942; b) M. H. J. Seifert, J. Georgescu, D. Ksiazek, P. Smialowski, T. Rehm, B. Steipe, T. A. Holak, *Biochemistry* **2003**, *42*, 2500 – 2512, and references therein.

[45] a) J. J. van Thor, A. J. Pierik, I. Nugteren-Roodzand, A. Xie, K. J. Hellingwerf, *Biochemistry* **1998**, *37* 16915 – 16921; b) J. J. Van Thor, T. Gensch, K. J. Hellingwerf, L. N. Johnson, *Nat. Struct. Biol.* **2002**, *9*, 37 – 41.

[46] a) A. F. Bell, D. Stoner-Ma, R. M. Wachter, P. J. Tonge, *J. Am. Chem. Soc.* **2003** *125*, 6919 – 6926, and references therein; b) P. Schellenberg, E. Johnson, A. P. Esposito, P. J. Reid, W. W. Parson, *J. Phys. Chem.* **2001**, *105*, 5316 – 5322, and references therein; c) S. G. Kruglik, V. Subramaniam, J. Greve, C. Otto, *J. Am. Chem. Soc.* **2002**, *124*, 10992 – 10993; d) S. Habuchi, M. Cotlet, R. Gronheid, G. Dirix, J. Michiels, J. Vanderleyden, F. C. De Schryver, J. Hofkens, *J. Am. Chem. Soc.* **2003**, *125*, 8446 – 8447; e) V. Tozzini, A. R. Bizzarri, V. Pellegrini, R. Nifosi, P. Giannozzi, A. Iuliano, S. Cannistraro, F. Beltram, *Chem. Phys.* **2003**, *287*, 33.

[47] a) V. Tozzini, R. Nifosi, *J. Phys. Chem. B* **2001**, *105*, 5797 – 5803; b) H-Y. Yoo, J. A. Boatz, V. Helms, J. A. McCammon, P. W. Langhoff, *J. Phys. Chem. B* **2001**, *105*, 2850 – 2857.

[48] a) D. W. Pierce, N. Hom-Booker, R. D. Vale, *Nature* **1997**, *388*, 338; b) R. M. Dickson, B. Cubitt, R. Y. Tsien, W. E. Moerner, *Nature* **1997**, *388*, 355 – 358; c) G. Jung, J. Wiehler, W. Göhde, J. Tittel, Th. Basché, B. Steipe, C. Bräuchle, *Bioimaging* **1998**, *6*, 54 – 61; d) J. Schaffer, A. Volkmer, G. Eggeling, V. Subramaniam, G. Striker, A. M. Seidel, *J. Phys. Chem. A* **1999**, *103*, 331 – 336; e) M. F. García-Parajó, M. Koopman, E. M. H. P. Van Dijk, V. Subramaniam, N. F. Van Hulst, *Proc. Natl. Acad. Sci. USA* **2001**, *98*, 14392 – 14397; f) M. Cotlet, J. Hofkens, S. Habuchi, G. Dirix, M. van - Guyle, J. Michiels, J. Vanderleyden, F. C. De Schryver, *Proc. Natl. Acad. Sci. USA* **2001**, *98*, 14398 – 14403; g) G. Chirico, F. Cannone, A. Diaspro, S. Bologna, V. Pellegrini, R. Nifosi, F. Beltram, *Phys. Rev. E* **2004**, *70*, 030901 – 1–30901 – 4, and references therein.

[49] a) A. Zumbusch, G. Jung, *Single Mol.* **2000**, *1*, 261 – 270; b) M. F. García-Parajó, J.-A. Veerman, R. Bouwhuis, R. Vallée, N. F. Van Hulst, *ChemPhysChem* **2001**, *2*, 347 – 360; c) W. E. Moerner, *J. Chem. Phys.* **2002**, *117*, 10925 – 10937.

[50] a) G. S. Harms, L. Cognet, P. H. M. Lommerse, G. A. Blab, Th. Schmidt, *Biophys. J.* **2001**, *80*, 2396 – 2408; b) G. S. Harms, L. Cognet, P. H. M. Lommerse, G. A. Blab, H. Kahr, R. Gamsjäger, H. P. Spaink, N. M. Soldatov, C. Romanin, T. Schmidt, *Biophys. J.* **2001**, *81*, 2639 – 2646, and references therein.

[51] a) U. Haupts, S. Mati, P. Schwille, W. W. Webb, *Proc. Natl. Acad. Sci. USA* **1998**, *95*, 13573 – 13578; b) F. Malvezzi-Campeggi, M. Jahnz, K. G. Heinze, P. Dittrich, P. Schwille, *Biophys. J.* **2001**, *81*, 1776 – 1785, and references therein.

[52] S. Bonsma, J. Gallus, F. Könz, R. Purchase, S. Völker, *J. Lumin.* **2004**, *107*, 203 – 212.

[53] F. Könz, R. Purchase, S. Bonsma, J. Gallus, S. Völker, *J. Lumin.* **2004**, *108*, 153 – 157.

[54] a) S. Völker in *Relaxation Processes in Molecular Excited States* (Ed.: J. Fünfschilling), Kluwer, Dordrecht, **1989**, pp. 113 – 242 and references therein; b) S. Völker, *Annu. Rev. Phys. Chem.* **1989**, *40*, 499 – 530, and references therein; c) T. M. H. Creemers, S. Völker in *Shpol'skii Spectroscopy and Other Site-Selection Methods* (Eds.: C. Gooijer, F. Ariese and J. W. Hofstraat), John Wiley & Sons, New York, **2000**, pp. 273 – 306 and references therein.

[55] F. T. H. den Hartog, J. P. Dekker, R. van Grondelle, S. Völker, *J. Phys. Chem. B* **1998**, *102*, 11007 – 11016.

[56] M. L. Groot, J. P. Dekker, R. van Grondelle, F. T. H. den Hartog, S. Völker, *J. Phys. Chem.* **1996**, *100*, 11488 – 11495.

[57] W. W. Ward, C. W. Cody, R. C. Hart, M. J. Cormier, *Photochem. Photobiol.* **1980**, *31*, 611 – 615.

[58] C. Seebacher, F. W. Deeg, C. Bräuchle, J. Wiehler, B. Steipe, *J. Phys. Chem. B* **1999**, *103*, 7728 – 7732.

[59] J. Wiehler, G. Jung, C. Seebacher, A. Zumbusch, B. Steipe, *ChemBioChem* **2003**, *4*, 1164 – 1171.

[60] A. A. Heikal, S. T. Hess, G. S. Baird, R. Y. Tsien, W. W. Webb, *Proc. Natl. Acad. Sci. USA* **2000**, *97*, 11996 – 12001.

[61] T. A. Schüttrigkeit, U. Zachariase, T. von Feilitzsch, J. Wiehler, J. von Hummel, B. Steipe, M. B. Michel-Beyerle, *ChemPhysChem* **2001**, *5*, 325 – 328.

[62] B. Lounis, J. Deich, F. I. Rosell, S. G. Boxer, W. E. Moerner, *J. Phys. Chem. B* **2001**, *105*, 5048 – 5054.

[63] a) Th. Förster, *Ann. Phys.* **1948**, *2*, 55; b) Th. Förster in *Modern Quantum Chemistry, Part III* (Ed.: O. Sinanoglu), Academic Press, New York, **1965**, 93.

[64] a) F. T. H. den Hartog, C. van Papendrecht, R. J. Silbey, S. Völker, *J. Phys. Chem. B* **1999**, *110*, 1010 – 1016; b) F. T. H. den Hartog, C. van Papendrecht, U. Störkel, S. Völker, *J. Phys. Chem. B* **1999**, *103*, 1375 – 1380.

[65] a) I.-J. Lee, J. M. Hayes, G. J. Small, *J. Chem. Phys.* **1989**, *91*, 3463 – 3469; b) J.-G. van der Toorn, M. Sc. Thesis, Leiden University, **1997**.

Received: January 4, 2005
Revised: March 7, 2005

